DOI: 10.2195/lj_Rev_siegel_en_201307_01
URN: urn:nbn:de:0009-14-37084

Energy and weight reduction in hoisting systems with magnetic traction sheaves

Armin Siegel
Martin Anders
Thorsten Schmidt

Chair of Logistics Engineering
Institute of Material Handling and Industrial Engineering
Faculty of Mechanical Science and Engineering
TU Dresden

At the Chair of Logistics Engineering, TU Dresden, a particular focus is research and development of magnetic traction sheaves. Therein the main fundamentals of these special sheaves are determined for applications in different fields such as elevators, several kinds of winches, hoists and cranes. In the current research project "energy balance of magnetic traction sheaves", the dynamic behaviour of systems with magnetic traction sheaves was investigated. The research focused on theoretical and practical examinations of energy balance. Moreover, a new approach for dimensioning magnetic traction sheave systems is presented. It is a project of the Research Foundation Intralogistics / Material Handling and Logistics (IFL), which is funded through the AiF under the program of Industrial Collective Research for SMEs (IGF) by the Federal Ministry of Economics and Technology (BMWi).

[Keywords: Magnetic Traction Sheave, Energy Balance, Elevator, Hoisting System, Mass Reduction]

An der Professur für Technische Logistik liegt ein Schwerpunkt auf der Erforschung und Entwicklung von Magnettreibscheiben. Dabei wurden die Grundlagen für die Verwendung der speziellen Treibscheiben in unterschiedlichen Anwendungsfeldern wie dem Aufzugbau, bei Seilwinden und Hebezeuge sowie dem Kranbau aufgezeigt. Das aktuelle Forschungsprojekt „Energiebilanz beim Einsatz von Magnettreibscheiben" untersucht das dynamische Verhalten von Systemen mit Magnettreibscheiben. Es stehen theoretische und praktische Untersuchungen bezüglich des Energieumsatzes im Mittelpunkt. Darüber hinaus wird ein neuer Ansatz Magnettreibscheiben auszulegen präsentiert. Das Projekt ist ein Vorhaben der Forschungsgemeinschaft Intralogistik / Fördertechnik und Logistiksysteme (IFL), das über die AiF im Rahmen des Programms zur Förderung der industriellen Gemeinschaftsförderung und -entwicklung (IGF) vom Bundesministerium für Wirtschaft und Technologie (BMWi) gefördert wird.

[Schlagworte: Magnettreibscheibe, Energiebilanz, Aufzug, Hebesystem, Massenreduktion]

1 MAGNETIC TRACTION SHEAVES

In their basic operation, magnetic traction sheaves (MTS) (cp. [1], [2]) are equal to conventional traction sheaves (CTS) applied in elevators, hoisting systems, mine hoists and cable cars (cp. figure 1).

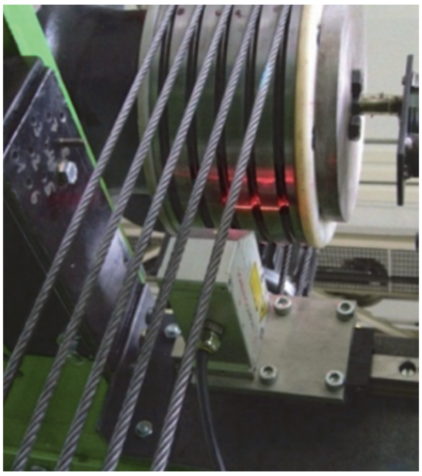

Figure 1. Magnetic traction sheave at the test bench

By using high performance NdFeB-magnets, an additional line load is generated which pulls the rope into the sheave groove and creates higher friction in the traction sheaves. This is possible because a magnetic circuit is closed by the wire rope and hence the total rope cross section is involved in increasing the traction capability. Earlier research found that the use of an undercut round groove in combination with the friction coefficient, groove pressure and traction capacity is the best solution for the highest magnetic effect [3]. Even due to lower groove pressure, the lifetime of the rope is increased by similar or higher traction capability compared to conventional sheaves with v-grooves. However, in contrast to conventional traction sheaves, the traction is not constant and depends on the rope load. For traction elevators with counterweight and according systems (cp. figure 2), the conditions are met to move a specific payload with the least inertia in the system.

DOI: 10.2195/lj_Rev_siegel_en_201307_01
URN: urn:nbn:de:0009-14-37084

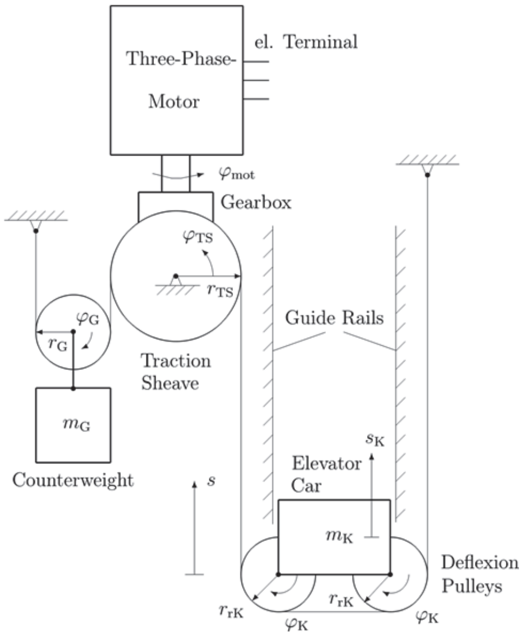

Figure 2. Elevator system

In this study, a mechanical model according to figure 3 based on Eytelwein's law (Belt friction) was built to compare the inertia in systems with MTS and CTS [3], [7].

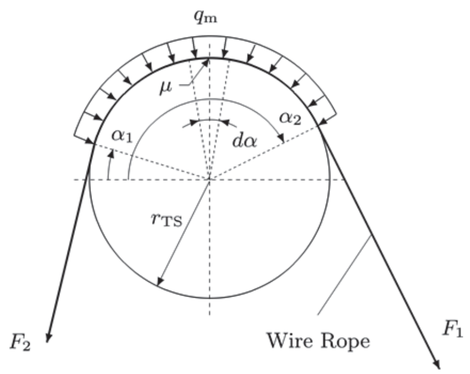

Figure 3. Magnetic traction sheave model

The additional magnetic force is modelled by a line load q_m. Hence the distributed traction capacity of the magnetic traction sheave (F_1/F_2) is described with:

$$e^{-\mu\alpha} + \frac{q_m\, r_{TS}\,(e^{-\mu\alpha}-1)}{F_2} \le \frac{F_1}{F_2} \le e^{\mu\alpha} + \frac{q_m\, r_{TS}\,(e^{\mu\alpha}-1)}{F_2} \qquad (1)$$

Therein angle of deflection $\alpha = \alpha_2 - \alpha_1$, friction coefficient μ and traction sheave radius r_{TS} are determined. In the case of conventional traction sheave systems the model sets q_m to zero.

2 COMPARISON OF THE TRACTION CAPACITY IN BOTH SYSTEMS

Equation (1) is suitable for a comparison of the two traction sheaves. Assuming a load-independent coefficient of friction, especially independent of the rope forces F_1 and F_2, the limits of the distributed traction capacity for conventional traction sheaves with $q_m = 0$ are two constant values. Using the convention that F_1 is larger, equation (1) results in the well-known simplified formula which is typically used in material handling:

$$\frac{F_1}{F_2} \le e^{\mu\alpha} \qquad (2)$$

To verify any allowed dimensioning, equation (1) is especially applicable for magnetic traction sheaves. Figure 4 shows an example of the traction capacity range for conventional and magnetic sheaves.

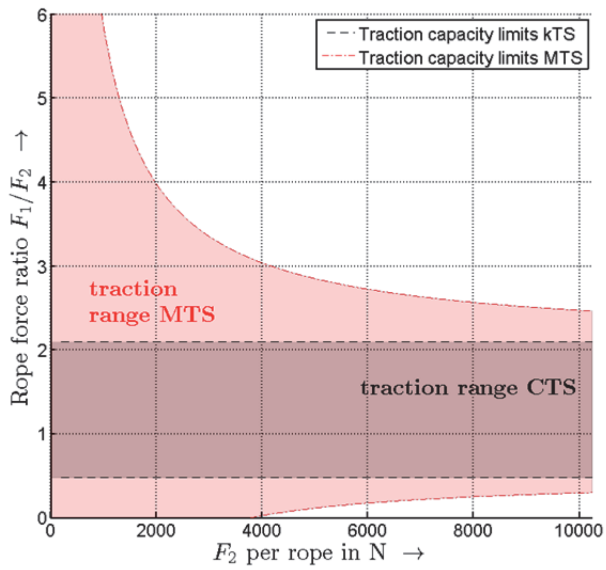

Figure 4. Comparison of the distributed traction capacity between conventional and magnetic traction sheaves

The rope force ratio F_1/F_2 over the force F_2 per rope is shown. For the conventional sheave with given deflection angle α and friction coefficient μ, a constant maximum distributed traction follows (see equation (2)). As mentioned, F_2 can be the larger rope force instead of F_1, which is different to common considerations in material handling technology. The inverse of equation (2) results in the displayed lower limit of the traction capacity. Analogously, the maximum and minimum limits are shown for the magnetic sheave and determined with equation (1). As a result, with the same deflection angle and friction coefficient, a larger range of traction capacity is distributed by the magnetic sheave. A prerequisite is a magnetic line load q_m larger than zero. The additional traction capacity depends on the cable load. Thus its influence on small rope force F_2 is larger than for large rope payloads according to each second term in equation (1). Therefore, the dimension of traction sheave driven systems should be examined to exploit this new behavior, and to design and demonstrate the potential in saving construction material and energy.

DOI: 10.2195/lj_Rev_siegel_en_201307_01
URN: urn:nbn:de:0009-14-37084

3 ENERGY BALANCE OF MTS

With the goal of creating a design tool for magnetic traction sheaves, research on the effects that occur between the magnetic traction sheave and the wire rope is relevant. The question arises; “Is more energy required during operation by the additional magnetic force on the wire rope?” In order to answer this question, the bending resistance and the influence of the magnetic field was examined at the entry and outlet of the traction sheave rope. Firstly, a FEM (finite element method) model and a multi-body model were created. Secondly, the additional rope deflection was determined in experiments and thirdly, the need of electrical power and energy for both traction sheaves was compared in power measurements.

The magnitude of magnetic forces was examined at the entry and outlet of the wire rope, where the rope leaves the traction sheave groove. This is of particular interest since the magnetic field pulls the wire rope for a certain extent into the groove beyond the theoretical disengagement. To use the finite element method, the behavior of the magnetic field was observed with increasing distance between the rope and rope groove. As a result, for the examined samples of magnetic traction sheaves, the magnetic field strength is very strong between the groove flanks. With increasing distance from the flanks, the field strength decreases. For example, in traction sheaves with a diameter of 240 mm the force effect decreases within an angle of 10 degrees. In consequence, the magnetic force acting on the rope in the entry and outlet area also decreases with the distance, as the determination of the magnetic force vectors from the static magnetic field analysis shows (see figure 5).

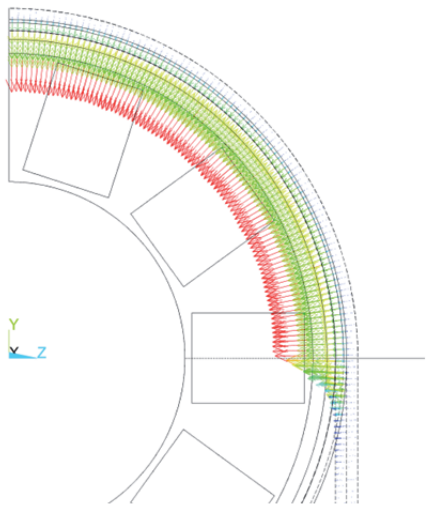

Figure 5. Sample of calculated magnetic force vectors between magnetic traction sheave and wire rope

The force effects are shown for a tangentially outbound rope. If additional rope bending occurs, the forces on the graph change, therefore, it was examined how much the cable bends under the rope force. Geometric measurements of small rope forces on magnetic sheaves show that the rope bend assumes large bending values only at low loads on the cable (cp. figure 6)

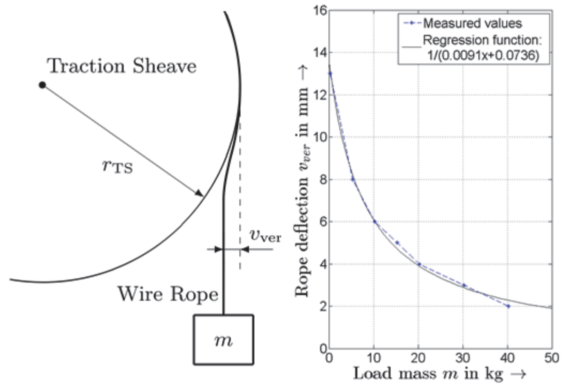

Figure 6. Experiment and result for the measurement of bending offset on magnetic traction sheave

For practical applications the low load range is irrelevant. As a result, the measured force effects of the tangential outbound rope are, in practice, achieved. In a traction sheave driven system a rope entry and outlet always work together simultaneously. With respect to the applied torque, the force effects in these areas compensate for torque balance as shown with a free-body model in figure 7.

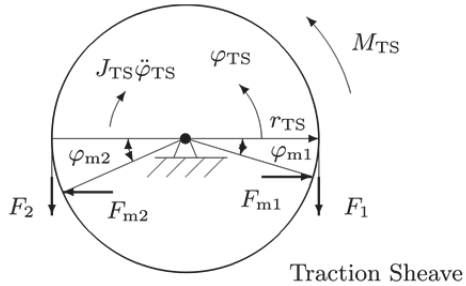

Figure 7. Free-body model of the MTS with added magnetic forces at rope entry and outlet

The relationships described here do not reflect increased energy consumption in the real system. To investigate practically relevant influences from the different bending resistance of the rope, power measurements were carried out on an elevator test system. To determine the mechanical or magnetic influences of the different sheaves, the electrical active power was measured directly between the frequency converter and the asynchronous motor. This was done to prevent influences of electrical losses in the inverter (see Figure 8).

The power was measured for geometrically identical sheaves provided with and without permanent magnets. Furthermore, the measurement was carried out with different load mass ratios and the respective force ratios. For comparability reasons the ratio selection happened so that each was conveyable by both sheaves.

DOI: 10.2195/lj_Rev_siegel_en_201307_01
URN: urn:nbn:de:0009-14-37084

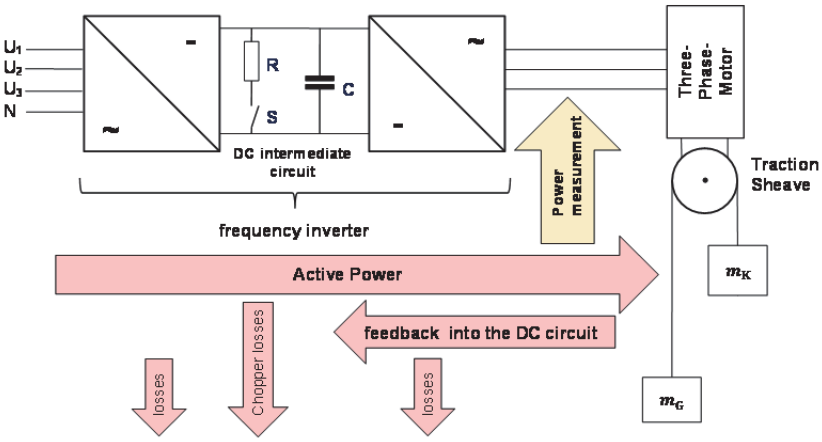

Figure 8. System design of test stand with place of *power measurement and marked power flow*

For the comparison afterwards, the integral of the measured power over several hoist cycles was applied. This value characterizes energy needed within both systems. The graph of the measured real power for one hoist cycle is of example shown in figure 9.

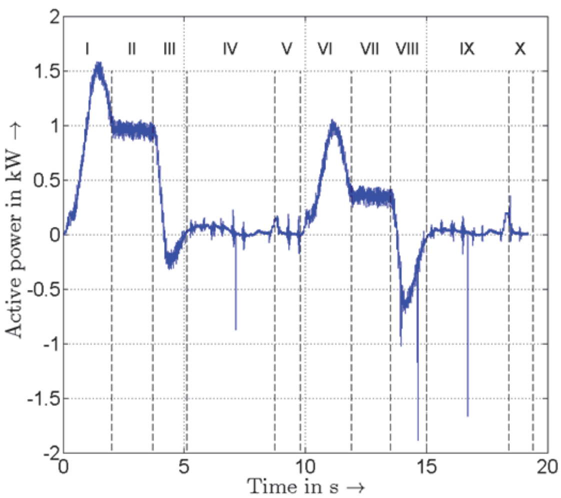

Figure 9. Graph of the measured power for one hoist cycle with the sections of: I - acceleration heavy side up; II - constant travel, III – deceleration, IV – leveling, V - stop, VI - acceleration light side up and so on.

The results, along with a statistical analysis show that for large loads practically no difference between the needed energy in a direct comparison could be measured (see table 1). As theoretically suspected above, no influence of the magnetic effect is seen with loads larger 50 kg, approximately 2 % of the minimum breaking force for the used 8 mm wire rope. This is confirmed by the overlap of confidence intervals of the measurements with load ratios 113 kg/95 kg and 132 kg/94 kg, and a confidence range of less than 2s (two times empirical standard deviation). For the load ratio 37 kg/37 kg confidence intervals do not intersect within this confidence range. The cause is suspected in the higher slip rate for the conventional traction sheave, especially at low rope loads or loads close to zero kilograms. This assumption is confirmed by marginally higher energy consumption during acceleration phases.

3.1 TOOL SUPPORTED DESIGN

As the previous discussion shows, the differences through the use of magnetic traction sheaves with respect to the energy balance in a direct comparison (with the same system parameters) are low or negligible. Moreover, the focus of the project was on the use of the increased traction capacity by the magnetic traction sheave. This led to the development of a design tool which allows the design of magnetic traction sheave driven systems.

Table 1. Consumed energy for conventional and magnetic traction sheave per hoist cycle and 8 repetitions

	Magnetic Traction Sheave (MTS)		**Conventional Traction Sheave (CTS)**		**Difference**
Mass ratio	Consumed energy in kWs	Standard-deviation in kWs	Consumed energy in kWs	Standard-deviation in kWs	MTS - CTS in kWs
37 kg/37 kg	4,185	0,021	4,326	0,020	-0,141
113 kg/95 kg	4,494	0,034	4,484	0,031	0,010
132 kg/94 kg	4,570	0,039	4,643	0,025	-0,073

DOI: 10.2195/lj_Rev_siegel_en_201307_01
URN: urn:nbn:de:0009-14-37084

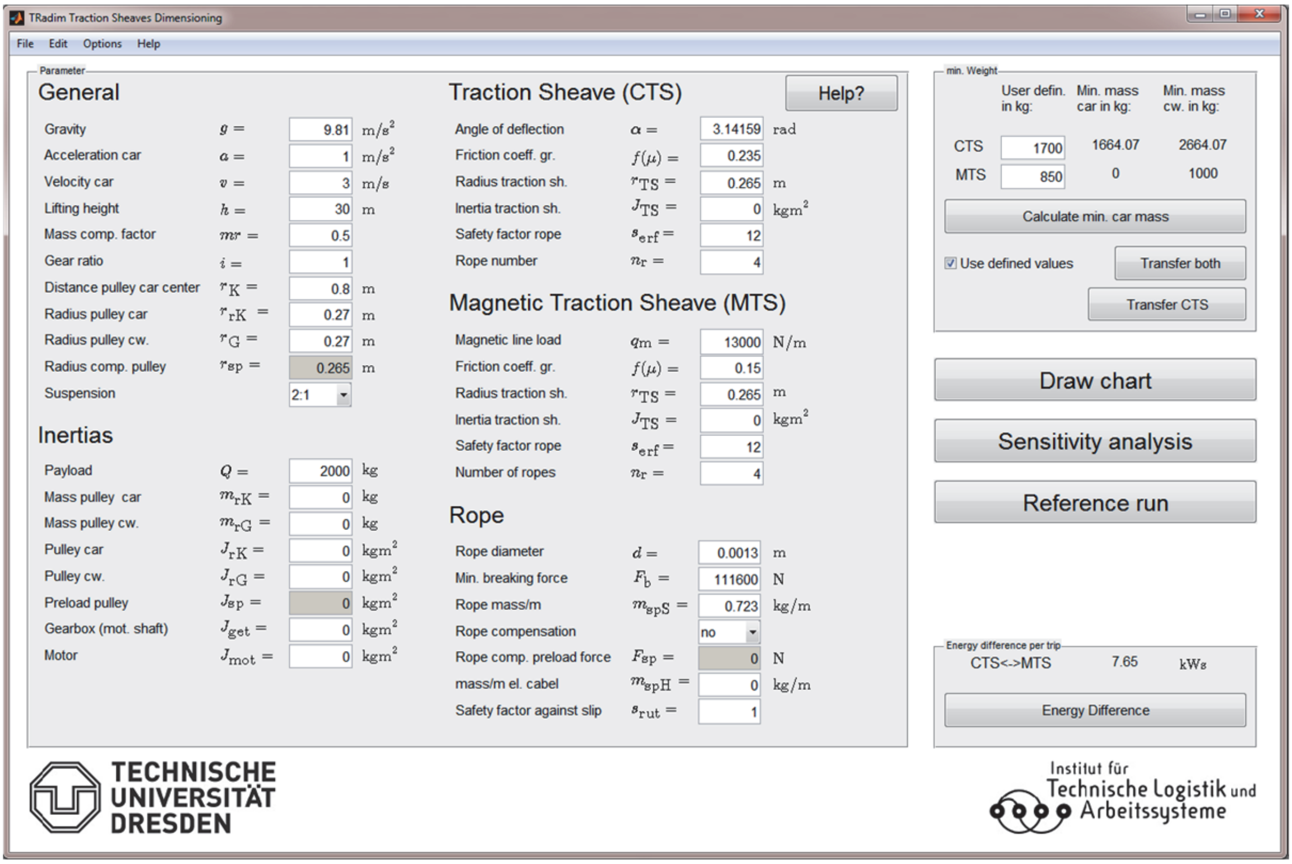

Figure 10. Screenshot of the programs graphical user interface (GUI)

Additionally it shows the difference to conventional systems. The program is written in Matlab® and based on the calculations and design regulations in DIN EN 81-1 [5] as well as TRA 003 [6] and the above presented equation (1).

Consequently, the parameter names are similar to the terms used in elevator engineering. Moreover, the approach can be applied to other traction sheave driven systems to ensure the traction capacity at varying rope loads. Figure 10 shows a screenshot of the graphical user interface (GUI) of the developed design tool.

In the program, elevator system parameters such as velocity, acceleration, inertia and geometric dimensions are considered. Furthermore, the input data for calculation of conventional traction sheaves and magnetic traction sheaves are specified separately to provide a comparison of systems with different numbers of ropes, groove shape (friction coefficient of groove) and required rope safety factor. It is also possible to select between 1:1 and 2:1 suspension. Optional balanced ropes can be considered. In the calculation, a maximum payload of 125 % was already used according to DIN EN 81-1. If desired, an additional safety factor against slipping of wire ropes at the traction sheave can be specified. After entering the data, the minimum weight for car and counterweight can be calculated or defined by the user. Finally it is possible to inspect and check the calculation by graphical visualization.

3.2 CALCULATION PRINCIPLE

Based on a free-body model of the elevator system, the rope forces F_1 and F_2 are determined. An example is shown in figure 11.

It is a reduced model for the consideration of rope, car and counterweight masses. The mass and inertia of pulleys and travelling cable to car electric energy supply are neglected.

Within the model gravitational acceleration g, car current position $s_K = s_G$, maximum lifting height h, car acceleration $\ddot{s}_K$, number of wire ropes n_r and specific rope mass m_{sp} are considered. The total car weight m_K consists of the mass of car P and current payload Q. On the other side, counterweight mass is the sum of cabin mass P and as defined by the mass compensation factor half of the maximum payload Q. As a result, both rope forces are given with the following equations:

$$F_1 = \left(\underbrace{m_K}_{P+Q} + 2m_{sp}n_r(h - s_K)\right)\left(\frac{g + \ddot{s}_K}{2}\right) \tag{3a}$$

DOI: 10.2195/lj_Rev_siegel_en_201307_01
URN: urn:nbn:de:0009-14-37084

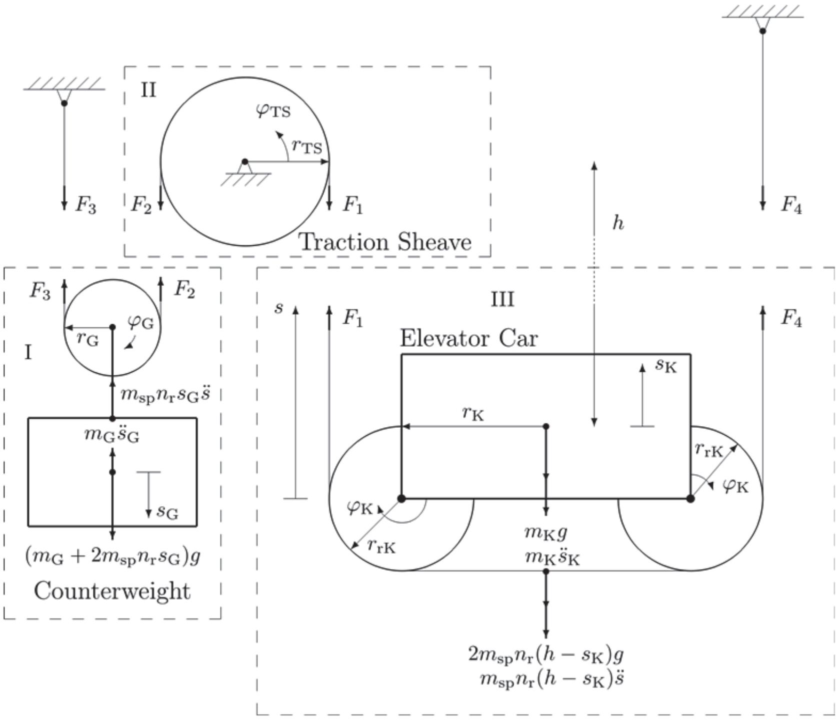

Figure 11. Free-body diagram of an elevator with 2:1 suspension

$$F_2 = \left(\underbrace{m_G}_{P+Q_{max}/2} + 2m_{sp} n_r s_K \right) \left(\frac{g - \ddot{s}_K}{2} \right) \tag{3b}$$

With the two forces the minimum mass, in conjunction with above presented equation (1) for traction capacity range, can be calculated (see also figure 3 and 11). It should be ensured that the rope forces from equations (3) are always within the traction capacity ranges. Consequently, the extreme values of the equations (3) have to be checked. F_1 takes its maximum for the lowest position

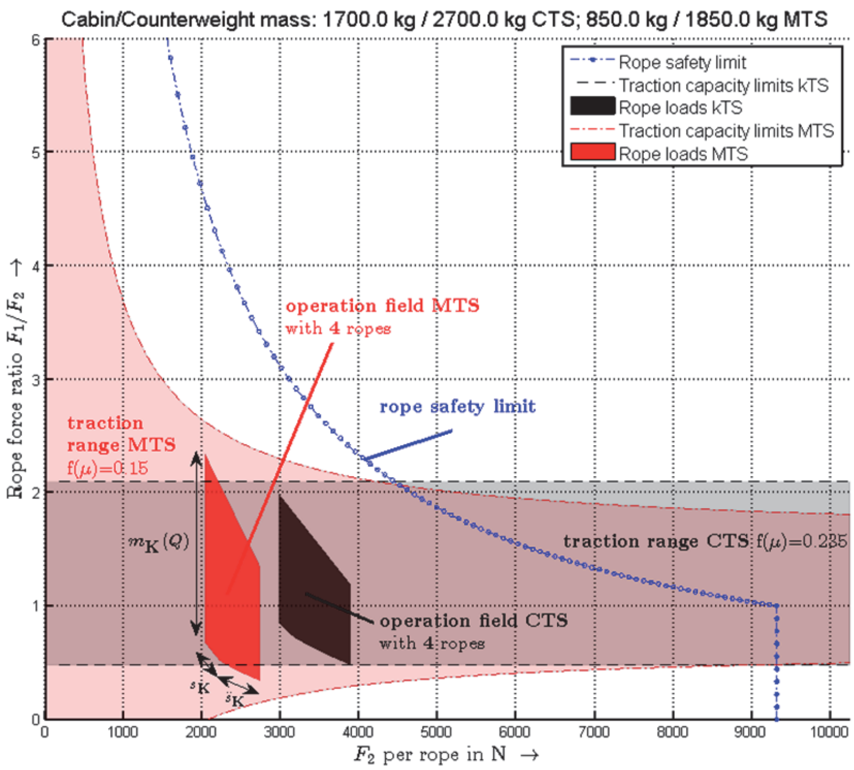

Figure 12. Conditions of the traction sheave systems for a 2:1 suspended elevator system with CTS and MTS

DOI: 10.2195/lj_Rev_siegel_en_201307_01
URN: urn:nbn:de:0009-14-37084

$s_K = 0$, the maximum acceleration $\ddot{s}_K = \ddot{s}_{Kmax}$ and the maximum payload $m_K = P + Q_{max}$. Its minimum results from $F_1(s_K = h;\ \ddot{s}_K = -\ddot{s}_{Kmax};\ m_K = P)$. Similarly, the maximum of F_2 results with $F_2(s_K = h;\ \ddot{s}_K = -\ddot{s}_{Kmax};\ m_G = P + Q_{max}/2)$ and the minimum with $F_2(s_K = 0;\ \ddot{s}_K = \ddot{s}_{Kmax};\ m_G = P + Q_{max}/2)$. Used in both parts of equation (1) and transposed separately for P, it results in two values for mass of car P. The larger one defines the minimum car mass. In other words the intersection of extreme values for the needed traction capacity F_1/F_2 and the traction capacity distributed by the traction sheave is calculated. The following example prepares this context graphically.

3.3 EXAMPLE FOR BOTH SYSTEMS IN COMPARISON

Figure 12 shows the program's evaluation for one elevator with classical and magnetic traction sheave. The forces ratio F_1/F_2 is displayed, depending on the rope force F_2 per cable (cp. figure 4). As illustrated above, it results in the ranges for both traction sheaves, in which a slip free operation for given input parameters is secured. Additionally, a limit line for ensuring rope safety is drawn, which was calculated from the necessary safety factor and the minimum rope breaking force.

From the input system parameters, including the calculated or given minimum masses (m_K, m_G), the forces F_1 and F_2 as described per rope at different percentages of the maximum payload Q_{max} (0-125 %), acceleration (±100 %) and lifting height (0-100 %) are calculated.

As result, for each sheave an operation field is presented that reflects all occurring rope force states. Thus the needed traction capacity as well as the necessary safety factor of the supporting ropes is ensured, the corresponding operation fields have to be within each distributed traction capacity range and under the mentioned rope safety limit. The above discussed extreme values of rope forces and the subsequently calculated needed traction capacity are reflected in the operation field corners (each top left and bottom right of operation field).

Figure 12 provides a fast and clear evaluation of how a traction sheave driven system is designed, and which reserves are available. Moreover, the main difference between conventional and magnetic traction sheaves becomes clear. This opened as a result, the use of the increased distributed traction capacity by magnetic traction sheaves.

The example shows a comparison of two elevator systems with the same payload of 2000 kg. In the conventional case a groove with v-groove angle γ = 45° and resulting friction coefficient of groove $f(\mu) = 0.235$ is expected. The magnetic traction sheave uses a value of $f(\mu) = 0.15$. In classical consideration, this would mean a lower traction capacity, with larger car and counterweight masses needed. As shown in figure 12, the masses for the conventional system are much higher with 1700 and 2700 kg, compared to the magnetic traction sheave with 850 and 1850 kg. In this example the theoretically smallest possible car mass of zero kilograms in the MTS system is not used for the calculations. So with the given masses it is allowable to adjust and reduce the car and counterweight mass as desired. In the theoretic example with car mass zero, the counterweight mass has to be adjusted to half of the maximum payload. The limiting factor is the production of a lightweight car and its cost. In table 2 the parameters listed are used in the calculation example shown in figure 12. For the car mass, instead of the conventional 1700 kg, a mass of 850 kg was taken. The magnetic force or line load used is defined on FEM calculations and experiments with 13 N/mm and can be regarded as a reliable and currently achievable magnitude practically. In general the value of this magnetic line load depends on used magnets, structural design of sheave components as well as structure of the applied wire rope.

Table 2. Parameter overview for the calculated example

	Conventional traction sheave (CTS)	**Magnetic traction sheave (MTS)**
System	Traction sheave elevator with 2:1 suspension, lift height $s_K = 30$ m, traction sheave diameter $r_{TS} = 265$ mm	
Groove shape/geometry	v-groove with angle γ = 45°	round groove with undercut angle α < 75°
Friction coefficient groove $f(\mu)$	0.235	0.15
Magnetic line load q_m	-	13 N/mm
Velocity $\dot{s}_{Kmax}$	3 m/s	
Acceleration car $\ddot{s}_{Kmax}$	±1 m/s²	
Rope	Minimum breaking force 111.6 kN, diameter 13 mm, specific weight m_{sp}=0.723 kg/m, rope safety factor 12	
Number of ropes n_r	4	4 (within the safety limit 3 possible)
Payload Q_{max}	2000 kg	2000 kg
Car weight P	1700 kg	850 kg (0 kg theoretically possible)
Counterweight $P + Q_{max}/2$	2700 kg	1850 kg
Weight savings (only car and counterweight)	0	1700 kg

DOI: 10.2195/lj_Rev_siegel_en_201307_01
URN: urn:nbn:de:0009-14-37084

In addition to the mass reduction, further savings arise as a result of the lower inertia in the system. For example with a car mass of 850 kg and four wire ropes the MTS operation field distance from required rope safety limit is high enough to reduce wire rope number (cp. figure 12). Therefore again increasing the stress per rope and the operation field of the MTS system moves in the diagram to the right. In this case an operation of the MTS system with only three support ropes would be possible (see figure 13).

Furthermore, the reduction of moving system masses has an impact on other components of an elevator system. Safety brake, guide rails, buffers, etc. can be of smaller dimensions which saves additional material and costs.

In addition, energy can be saved. For determination of the amount, the potential and kinetic energy needed in CTS and MTS system is considered.

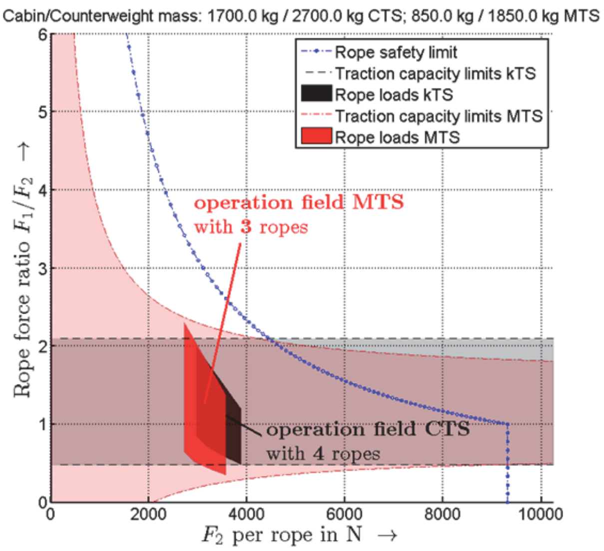

Figure 13. Example with reduced number of wire ropes in MTS system

The potential energy results with the mass m_{pot} and height h_{pot} in the known formula:

$$E_{\text{pot}} = m_{\text{pot}} \cdot g \cdot h_{\text{pot}}. \tag{4}$$

Explained by the counterweight principle, only the difference of the masses on car and counterweight side causes a change of potential energy need. The potential energy for the reduced model (cp. equation (3) and paragraph 3.2) is given with the formula:

$$E_{pot} = g\left(\left(Q - \frac{Q_{\max}}{2}\right) s_{\text{K}} + m_{\text{sp}} n_{\text{r}}(h^2 + 2hs_{\text{K}} - 2s_{\text{K}}^2)\right). \tag{5}$$

It depends on the current position s_{K}, the maximum $Q_{\max}$ as well as current payload Q and the kind m_{sp} and number n_r of wire ropes. The main effect is caused by the payload in combination with the counterweight balancing $Q_{\max}/2$. In comparison of CTS and MTS systems these parameters are the same. Ropes potential energy represented by the second term in equation (5) has its maximum at half of maximum lifting height and minimum at the car down and upside position. Conclusion is that less energy is needed with a smaller wire rope number during movement from the car down and upside position to half of the lifting height ($gm_{\text{sp}}n_{\text{r}}h^2/4$ in the example approximately 1.6 kWs = 0.44 Wh). The same amount of energy provides the system with less ropes in opposite movements out of position $s_{\text{K}} = h/2$. As a result there is no difference in potential energy consumption by changing the car mass and a small difference in consumption or recovery depending on the current movement by reducing the number of wire ropes. If complete hoisting cycles are considered, the potential energy has not a significant effect.

A different behavior shows the kinetic energy because the total mass in the systems has to be accelerated. The kinetic energy is calculated with mass m_{kin} and velocity v_{kin}:

$$E_{\text{kin}} = \frac{m_{\text{kin}}}{2}\, v_{\text{kin}}^2. \tag{6}$$

For the reduced model results:

$$E_{\text{kin}} = \frac{2\text{P}+\text{Q}+\text{Q}_{\max}}{2}\, \dot{s}_{\text{Kmax}}^2 + \frac{\text{m}_{\text{sp}} n_{\text{r}} h}{2}(2\dot{s}_{\text{Kmax}})^2. \tag{7}$$

In this calculation the car mass has a significant and the number of wire ropes a smaller impact on the kinetic energy. The difference between CTS and MTS system is given with:

$$\Delta E_{\text{kin}} = \Delta\text{P}\, \dot{s}_{\text{Kmax}}^2 + \frac{\text{m}_{\text{sp}}\, \Delta n_{\text{r}} h}{2}(2\dot{s}_{Kmax})^2. \tag{8}$$

In the presented example ΔE_{kin} is 8.04 kWs (7.65 and 0.39 kWs), approximately 2.2 Wh, and could be saved during each acceleration process depending on the actual amount of potential energy. With the developed design tool it is possible to compare a reference run, described in VDI 4707 (complete hoisting cycle down, up and down). It allows evaluating the superposition of potential and kinetic energy at the used load states. Moreover the difference in needed energy per acceleration as described can be calculated and obtained without the consideration of efficiencies. Whereas, in an idealized system only energy savings occur, if the system is one without energy recovery, because braking or recuperation states have to considered.

If efficiencies are included, especially in energetic recovered elevators, energy savings are expected by the system with MTS. These energy savings affects operating costs per year depending on the traffic levels.

DOI: 10.2195/lj_Rev_siegel_en_201307_01
URN: urn:nbn:de:0009-14-37084

For example with the VDI 4707 defined payload states of 0, 25, 50, 75 and 100 % of the maximum payload, energy savings occur in a not recovery systems with 50 and 75 % of load. According to VDI 4707 these payload states have each a total trip ratio of 10 %. As result in 20 % of all trips the described energy savings occur. Depending on the trips per year the energy savings could calculated. An elevator with 200 000 trips per year saves almost 90 kWh per year. Overall energy savings for on year are small compared with rope and mass savings.

4 CONCLUSION

The presented examination shows by the use of magnetic traction sheaves that material as well as energy and others savings are reached (1700 kg and one wire rope in the sample). Through the consideration of the described dynamic behavior especially for magnetic traction sheave systems, from the proposed suggestion by the inventor of the magnetic traction sheave [1], a significant advance in the findings for the qualification is determined. With the described dimensioning approach it is possible to design and evaluate traction sheave systems with counterweight and MTS. The illustrations within the developed design tool also provide the base to promote lightweight constructions in traction sheave driven systems. Altogether the result enables the industrial use of magnetic traction sheaves with the vision of resource efficient and therefore more sustainable vertical transport processes.

REFERENCES

[1] Gräbner, P.: *Neue Wege bei der Anwendung des Leichtbaus in der Aufzugstechnik, Die Magnettreibscheibe als Basis leichter Konstruktionen* In: Hebezeuge Fördermittel – Fachzeitschrift für Technische Logistik, Berlin 48 (2008) 5., S. 356-359

[2] Gräbner, P.: *Treibscheibe für Hochleistungsreibpaarungen.* Patent WO 03/ 076324 A 1, 7. March 2003.

[3] Leonhardt, T.; Herhold, R.*: Einsatz von Magnettreibscheiben zur Erhöhung der Treibfähigkeit.* Tagungsband zur 16. Internationalen Kranfachtagung, Magdeburg, O.-v.-Guericke-Univ., 2008, S. 109-121.

[4] Herhold, R.; Anders, M.; Schmidt, T.: *Entwicklung optimierter mehrrilliger Treibscheiben für Aufzüge.* In: Scheid, Wolf-Michael (Hrsg.): 5. Fachkolloquium der Wissenschaftlichen Gesellschaft für Technische Logistik (WGTL), 2009, S. 59-72 - ISBN 978-3-939473-56-5.

[5] DIN EN 81-1: *Safety rules for the construction and installation of lifts – Part 1: Electric lifts;* German version EN 81-1:1998+A3:2009: June 2010

[6] TRA 003: *Technische Regeln für Aufzüge. Berechnung der Treibscheibe. Deutscher Aufzugsausschuss (DAA).* 1981, ISBN 9783410205630.

[7] Schmidt, T.; Leonhardt, T.; Anders, M.: *Multiple-Grooved Magnetic Traction Sheaves.* In: Progress in Material Handling Research: 2010.

[8] VDI 4707: *Lifts energy efficiency. Part 1* March 2009.

The IGF project 16571 BR / 1 of the Research Foundation Intralogistics / Material Handling and Logistics (FG IFL) Lyoner Strasse 18, 60528 Frankfurt am Main is funded through the AiF under the program of Industrial Collective Research for SMEs (IGF) by the Federal Ministry for Economics and Technology, following a decision of the German Bundestag.

DOI: 10.2195/lj_Rev_siegel_en_201307_01
URN: urn:nbn:de:0009-14-37084

Dipl.-Ing. Armin Siegel, M.Sc., Research Assistant at the Chair of Logistics Engineering, Institute of Material Handling and Industrial Engineering, TU Dresden

Armin Siegel studied mechatronics at the TU Dresden from 2003 and completed his diploma degree at Chair of Laser and Surface Technology in cooperation with the Robert Bosch GmbH in 2009. His thesis topic was: "Distance measurement for ultra-short laser pulse micromachining with galvano scanner system". Meanwhile he did internships at the Robert Bosch GmbH in Stuttgart, Germany and the Bosch Corporation Japan in Higashimatsuyama, Japan. In 2009 Armin Siegel started his Master of industrial engineering and management at the TU Dresden, and received his degree with the thesis "Assessment of energy consumption and life cycle costs for hoisting devices with magnetic traction sheaves". Since 2012 he has been working as research assistant at the Chair of Logistics Engineering. His research focus lies in the area of energy efficiency in Logistics.

Address: Technische Universität Dresden, Faculty of Mechanical Science and Engineering, Institute of Material Handling and Industrial Engineering, Chair of Logistics Engineering, 01062 Dresden Germany,
Phone: +49 351 463 34176,
Fax: +49 351 463 35499,
E-Mail: Armin.Siegel@tu-dresden.de

Dipl.-Ing. Martin Anders, Research Assistant at the Chair of Logistics Engineering, Institute of Material Handling and Industrial Engineering, TU Dresden

Martin Anders studied mechanical engineering between 2002 an 2009. After an internship at the Kirow Leipzig KE Kranbau Eberswalde AG he wrote at the Chair of Logistics Engineering his diploma thesis with the topic “Design and development of multiple-grooved magnetic traction sheaves”. From 2009 he works as research assistant at the Chair of Logistics Engineering and researches especially in the field of running wire ropes, its lifetime calculations and forecasts. Furthermore, Martin Anders has been contributing in the TSU e. V. (Association for Technical Safety and Environmental Protection) in the working group of supporting structures for dynamic loads.

Address: Technische Universität Dresden, Faculty of Mechanical Science and Engineering, Institute of Material Handling and Industrial Engineering, Chair of Logistics Engineering, 01062 Dresden Germany,
Phone: +49 351 463 39207,
Fax: +49 351 463 35499,
E-Mail: Martin.Anders@tu-dresden.de

Prof. Dr.-Ing. Thorsten Schmidt, Head of the Chair of Logistics Engineering, Director of the Institute of Material Handling and Industrial Engineering, TU Dresden

Thorsten Schmidt is full professor at the TU Dresden and heads the Chair of Logistics Engineering in the Mechanical Engineering faculty since 2008. He holds a diploma degree in mechanical engineering from the TU Dortmund and a Master degree in industrial engineering from the Georgia Institute of Technology. He received his Ph.D. from the TU Dortmund in 2001. His research areas are the design and optimization of facility logistics and production systems including a focus on the machinery and components involved. He currently works on energy efficient control strategies in material flow, fast approximation in early planning stages by means of standard design modules, on-line data analysis, formal verification of control logic, performance analysis of de-central and self-controlled systems, lightweight structures in material handling and stress analysis on wire ropes and toothed belts, respectively.

Address: Technische Universität Dresden, Faculty of Mechanical Science and Engineering, Institute of Material Handling and Industrial Engineering, Chair of Logistics Engineering, 01062 Dresden Germany,
Phone: +49 351 463 32538,
Fax: +49 351 463 35499,
E-Mail: Thorsten.Schmidt@tu-dresden.de